

# An Aggregate Model for the Particle Size Distribution in Saturn's Rings

Nikolai Brilliantov<sup>1</sup>, Pavel Krapivsky<sup>2</sup>, Hisao Hayakawa<sup>3</sup>, Anna Bodrova<sup>1,4,5</sup>, Frank Spahn<sup>5</sup> and Jürgen Schmidt<sup>5</sup>

<sup>1</sup>Department of Mathematics, University of Leicester, LE1 7RH UK.

<sup>2</sup>Department of Physics, Boston University, Boston, MA 02215, USA.

<sup>3</sup>Yukawa Institute for Theoretical Physics, Kyoto University, Sakyo-ku, Kyoto, Japan

<sup>4</sup>Department of Physics, Moscow State University, Moscow, Russia.

<sup>5</sup>Institut für Physik und Astronomie, Universität Potsdam, Germany

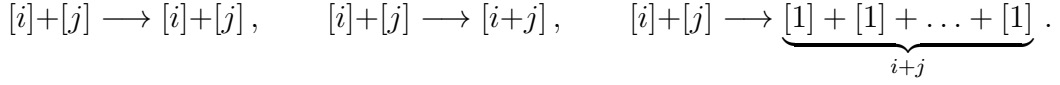
Saturn's rings are known to consist of a large number of water ice particles. They form a flat disk, as the result of an interplay of angular momentum conservation and the steady loss of energy in dissipative particle collisions. For particles in the size range from a few centimeters to about a few meters a power law distribution of radii  $\sim r^{-q}$ , with  $q \approx 3$ , is implied by the light scattering properties of the rings [1, 2, 3, 4]. In contrast, for larger sizes the distribution drops steeply [5, 6, 7, 8] with increasing  $r$ . It has been suggested that this size distribution may arise from a balance between aggregation and fragmentation of ring particles [9, 10, 11, 12, 13, 14, 15] but to date neither the power-law dependence, nor the upper size-cutoff have been explained or quantified within a unique theory. Here we present a new kinetic model for the collisional evolution of the size distribution and show that the exponent  $q$  is expected to be constrained to the interval  $2.75 \leq q \leq 3.5$ . An exponential cutoff towards larger particle sizes establishes naturally, the cutoff-radius being set by the relative frequency of aggregating and disruptive collisions. This cutoff is much smaller than the typical scale of micro-structure seen in Saturn's rings ( $\sim 100\text{m}$  for self-gravity wakes) [16] and our theory represents values averaged over these structures.

A short life-time of Saturn's rings to various evolutionary processes [17, 18, 19] indicates that ring particles and their size distribution may in fact not be primordial but are involved in an active accretion-destruction dynamics[20].

Tidal forces fail to explain the abrupt decay of the size distribution for large particles (Supplementary Information) and it is not clear, whether the observed size distribution is peculiar for Saturn’s rings, or if it is universal for planetary rings in general. Here we explain and quantify the reported properties of the size distribution within a kinetic aggregate model, based solely on the hypothesis of *binary* collisions of ring particles and the classification of the possible outcome of collisions as aggregative, restitutive, or disruptive. We quantify the rate of either collision type, depending on the collision speed, using the kinetic theory of granular gases[21] applied to a multi-sort system.

Ring particles may be imagined as “dynamic ephemeral bodies”[11], built up of primary grains[13] of a certain size  $r_0$  and mass  $m_0$ . Let the concentration of ring particles of size  $k$ , containing  $k$  primary grains, be  $n_k$ . In the kinetic approach (Supplementary Information) these particles are again assumed to be spherical, having mass  $m_k = k m_0$  and radius  $r_k = r_0 k^{1/3}$ . Dense rings composed of hard spheres can be described in the framework of the Enskog-Boltzmann theory [22, 23, 24]. In this case the rate of binary collisions depends on particle dimension and relative velocity. Namely, the cross-section for the collision of particles of size  $i$  and  $j$  scales as  $r_0^2(i^{1/3} + j^{1/3})^2$ , while the relative speed, being of the order of[4]  $0.01 - 0.1 \text{ cm/s}$ , is determined by the velocity dispersions  $\langle V_i^2 \rangle$  and  $\langle V_j^2 \rangle$  for particles of size  $i$  and  $j$ , respectively. The velocity dispersion quantifies the root mean square deviation of particle velocities from the orbital speed ( $\sim 20 \text{ km/s}$ ). These deviations follow a certain distribution, implying a range of inter-particle impact speeds, and thus, different collisional outcomes. The detailed analysis of an impact (Supplementary Information) shows that for collisions at small relative velocity, or small relative kinetic energy  $E$ , smaller than a certain threshold energy  $E_{\text{agg}}$  (determined by adhesion alone), particles stick together to form a joint aggregate. This occurs because adhesive forces acting between particle surfaces are strong enough to keep them together. For larger velocities particles rebound with a partial loss of their kinetic energy. For still larger impact speeds the relative kinetic energy exceeds the threshold energy for fragmentation,  $E_{\text{frag}}$  (again determined by the adhesion only), and particles break into pieces. Let  $\nu_{ij}$  be the collision rate (the number of collisions per unit time in a unit volume) for particles of size  $i$  and  $j$ . Only a fraction of these collisions, say,  $\lambda_{\text{agg}}\nu_{ij}$  leads to the formation of an aggregate of size  $(i + j)$ . Similarly, only the fraction  $\lambda_{\text{frag}}\nu_{ij}$ , leads to fragmentation of particles. If the

threshold energies  $E_{\text{agg}}$  and  $E_{\text{frag}}$  are some effective constant (Supplementary Information), the factors  $\lambda_{\text{agg}}$ ,  $\lambda_{\text{frag}}$  and  $\lambda \equiv \lambda_{\text{frag}}/\lambda_{\text{agg}}$ , characterizing the ratio of aggregative and disruptive collisions are constant as well. To illustrate the approach we consider here a simplified collision model, assuming that both particles break completely into monomers in a disruptive collision. A more general fragmentation model, with a particular distribution of debris size, gives essentially the same result if small fragments dominate (that is, size slope of fragments  $\geq 4$ ) (Supplementary Information). Schematically, we represent restitutive, aggregative and disruptive collisions as



The collision rate  $\nu_{ij} \propto n_i n_j$  is proportional to the concentrations of the colliding species,  $n_i$  and  $n_j$ . Then, with the notations,  $\lambda_{\text{agg}} \nu_{ij} = C_{ij} n_i n_j$  and  $\lambda_{\text{frag}} \nu_{ij} = \lambda C_{ij} n_i n_j$ , we write the evolution equation following from kinetic theory for the concentration of particles of size  $k > 1$ ,

$$\frac{dn_k}{dt} = \frac{1}{2} \sum_{i+j=k}^{\infty} C_{ij} n_i n_j - \sum_{i=1}^{\infty} C_{ik} n_i n_k - \lambda \sum_{i=1}^{\infty} C_{ik} n_i n_k. \quad (1)$$

Here the first term in the right hand side describes the rate at which aggregates of size  $k$  are formed in aggregative collisions of particles  $i$  and  $j$ . By conservation of mass, the summation extends over all  $i$  and  $j$  with  $i + j = k$ , and the factor  $\frac{1}{2}$  avoids double counting. The other two terms give the rate at which the particles of size  $k$  disappear in collisions with other particles of any size  $i$ , due to aggregation (second term) or fragmentation (third term). The restitutive collisions do not enter the above equation, since they do not alter the concentration of different species. A similar equation may be written for the evolution of monomers (Supplementary Information).

The rate coefficients  $C_{ij}$  and the constant  $\lambda$  in Eq. (1) are found from kinetic theory as functions of particles sizes  $i$  and  $j$  and threshold energies  $E_{\text{agg}}$  and  $E_{\text{frag}}$  (Fig. 1 and Supplementary Information). Moreover, we find that these coefficients are self-similar, namely,

$$C_{ai,aj} = a^{2\mu} C_{ij}, \quad (2)$$

which means that re-scaling of particle size by a factor  $a$  leaves the form of these coefficients unchanged. The constant  $\mu$  depends on the kinetic model

used for the ring particles: If all species have the same average kinetic energy  $\langle E \rangle = \langle \frac{1}{2} m_i V_i^2 \rangle$ , the scaling coefficient reads,  $\mu = \frac{1}{12}$ . The opposite case of equal velocity dispersion  $\langle V^2 \rangle = \langle V_i^2 \rangle$ , implies  $\mu = \frac{1}{3}$ . In reality, planetary rings are in state that is intermediate between these two cases. Indeed, the steady state velocity dispersion establishes as a balance of collisional cooling and shear heating, leading presumably to a fairly flat decrease of velocity dispersions with particle size, rather than to the energy equipartition[25]. Hence,  $\frac{1}{12} < \mu < \frac{1}{3}$  is expected.

Systems governed by kinetic equations of the form (1), with self-similar coefficients, have the important feature that their solution is mainly determined by the degree of homogeneity  $\mu$ , but not by the particular form[26] of  $C_{ij}$ . This allows us to use simplified coefficients  $C_{ij} = C_0 (ij)^\mu$ , with the same homogeneity exponent  $\mu$  and to find an analytical solution to Eqs. (1). The complete solution is involved (Supplementary Information). However, in the limit  $\lambda \ll 1$ , corresponding physically to rare fragmentation events, the steady-state solution has the simple form

$$n_k \sim k^{-(3/2+\mu)} e^{-\lambda^2 k/4}, \quad (3)$$

To obtain the radii distribution  $f(R)$ , which is constrained by observations, we use  $k \sim r_k^3 = R^3$  for spherical ring particles and obtain

$$f(R) \sim R^{-q} e^{-(R/R_c)^3}, \quad q = 5/2 + 3\mu, \quad R_c^3 = 4r_0^3/\lambda^2. \quad (4)$$

For  $R \ll R_c$  the distribution obeys a power-law with the exponent  $q = 5/2 + 3\mu$ ; for larger radii,  $R \sim R_c$ , it has an exponential cutoff.

Two important conclusions follow from this result. First, for the models of particle kinetics we study, the power-law exponent  $q$  varies within the interval  $2.75 \leq q \leq 3.5$ . Namely, for the limiting model where the average kinetic energy is the same for all particles, independently of their size,  $\mu = \frac{1}{12}$ , and we find  $q = 2.75$ . For the model where the velocity dispersion is the same for all species,  $\mu = \frac{1}{3}$  and  $q = 3.5$ . Naturally, these are two extreme cases and the ring particles must demonstrate an intermediate behavior, which corresponds to the above interval for  $q$ . Generally, the size slopes obtained from observations[2, 3] consistently lie in this interval, varying between  $q_{\text{obs}} = 2.74$  and  $3.11$ . Figure 1 shows a comparison of the theory to the particle size distribution derived for a part of Saturn's A ring[2]. Both theoretical and observational distributions represent an average over local small-scale ( $\sim 100\text{m}$ ) ring structure (Supplementary Information).

The second conclusion refers to the exponential cutoff of the distribution (4). It arises as a direct consequence of the competing fragmentation and aggregation processes, so that no other external mechanism is needed. The cutoff size,  $R_c$  is completely determined by the value of  $\lambda$ , which depends on the aggregation and fragmentation energies  $E_{\text{agg}}$  and  $E_{\text{frag}}$  (Fig. 1), and the minimal particle size  $r_0$  (Eq. 4). A fit to observations (Fig. 1) gives  $R_c = 5.6 m$ . Using  $R_c$ , our theory allows to constrain the size  $r_0$  of primary grains if the value of the average random velocity  $\bar{V}$  is known (Fig. 1 and Supplementary Information). A cutoff radius of  $R_c = 5.6 m$  is consistent with  $r_0$  in the range of  $0.1 - 5 \text{ cm}$  for average random velocities  $\bar{V}$  from the interval  $0.01 - 0.1 \text{ cm/s}$ , again in agreement with the observations[2, 4, 27].

## References

- [1] Marouf, E. A., Tyler, G. L., Zebker, H. A., Simpson, R. A. & Eshleman, V. R. Particle size distributions in Saturn's rings from Voyager 1 radio occultation. *Icarus* **54**, 189–211 (1983).
- [2] Zebker, H. A., Marouf, E. A. & Tyler, G. L. Saturn's rings - Particle size distributions for thin layer model. *Icarus* **64**, 531–548 (1985).
- [3] French, R. G. & Nicholson, P. D. Saturn's Rings II. Particle sizes inferred from stellar occultation data. *Icarus* **145**, 502–523 (2000).
- [4] Cuzzi, J. *et al.* *Ring Particle Composition and Size Distribution*, 459–509 (Springer, 2009).
- [5] Zebker, H. A., Tyler, G. L. & Marouf, E. A. On obtaining the forward phase functions of Saturn ring features from radio occultation observations. *Icarus* **56**, 209–228 (1983).
- [6] Tiscareno, M. S. *et al.* 100-metre-diameter moonlets in Saturn's A ring from observations of 'propeller' structures. *Nature* **440**, 648–650 (2006).
- [7] Sremcevic, M. *et al.* A Belt of Moonlets in Saturn's A ring. *Nature* **449**, 1019–1021 (2007).
- [8] Tiscareno, M. S., Burns, J. A., Hedman, M. M. & Porco, C. C. The Population of Propellers in Saturn's A Ring. *The Astronomical Journal* **135**, 1083–1091 (2008).

- [9] Harris, A. W. Collisional breakup of particles in a planetary ring. *Icarus* **24**, 190–192 (1975).
- [10] Davis, D. R., Weidenschilling, S. J., Chapman, C. R. & Greenberg, R. Saturn ring particles as dynamic ephemeral bodies. *Science* **224**, 744–747 (1984).
- [11] Weidenschilling, S. J., Chapman, C. R., Davis, D. R. & Greenberg, R. Ring particles - Collisional interactions and physical nature. In *Planetary Rings*, 367–415 (1984).
- [12] Gorkavyi, N. & Fridman, A. M. *Astronomy Letters* **11**, 628 (1985).
- [13] Longaretti, P. Y. Saturn’s main ring particle size distribution: An analytic approach. *Icarus* **81**, 51–73 (1989).
- [14] Canup, R. M. & Esposito, L. W. Accretion in the Roche zone: Coexistence of rings and ring moons. *Icarus* **113**, 331–352 (1995).
- [15] Spahn, F., Albers, N., Sremcevic, M. & Thornton, C. Kinetic description of coagulation and fragmentation in dilute granular particle ensembles. *Europhysics Letters* **67**, 545–551 (2004).
- [16] Colwell, J. E. *et al.* *The Structure of Saturn’s Rings*, 375 (Springer, 2009).
- [17] Cuzzi, J. N. & Durisen, R. H. Bombardment of planetary rings by meteoroids - General formulation and effects of Oort Cloud projectiles. *Icarus* **84**, 467–501 (1990).
- [18] Colwell, J. E. The disruption of planetary satellites and the creation of planetary rings. *Planetary and Space Science* **42**, 1139–1149 (1994).
- [19] Cuzzi, J. N. *et al.* An Evolving View of Saturn’s Dynamic Rings. *Science* **327**, 1470–1475 (2010).
- [20] Esposito, L. *Planetary Rings* (2006).
- [21] Brilliantov, N. V. & Pöschel, T. *Kinetic Theory of Granular Gases* (Oxford University Press, Oxford, 2004).

- [22] Araki, S. & Tremaine, S. The dynamics of dense particle disks. *Icarus* **65**, 83–109 (1986).
- [23] Araki, S. The dynamics of particle disks. II. Effects of spin degrees of freedom. *Icarus* **76**, 182–198 (1988).
- [24] Araki, S. The dynamics of particle disks III. Dense and spinning particle disks. *Icarus* **90**, 139–171 (1991).
- [25] Salo, H. Numerical simulations of dense collisional systems: II. Extended distribution of particle size. *Icarus* **96**, 85–106 (1992).
- [26] Leyvraz, F. Scaling theory and exactly solved models in the kinetics of irreversible aggregation. *Physics Reports* **383**, 95–212 (2003).
- [27] Schmidt, J., Ohtsuki, K., Rappaport, N., Salo, H. & Spahn, F. *Dynamics of Saturn’s Dense Rings*, 413–458 (Springer, 2009).

**Supplementary Information** is available.

We acknowledge discussions with Larry Esposito, Heikki Salo and Miodrag Sremčević. This work was supported by Deutsches Zentrum für Luft und Raumfahrt, Deutsche Forschungsgemeinschaft and by Russian Foundation for Basic Research (RFBR, project 12-02-31351). Numerical calculations were performed using Chebyshev supercomputer of Moscow State University.

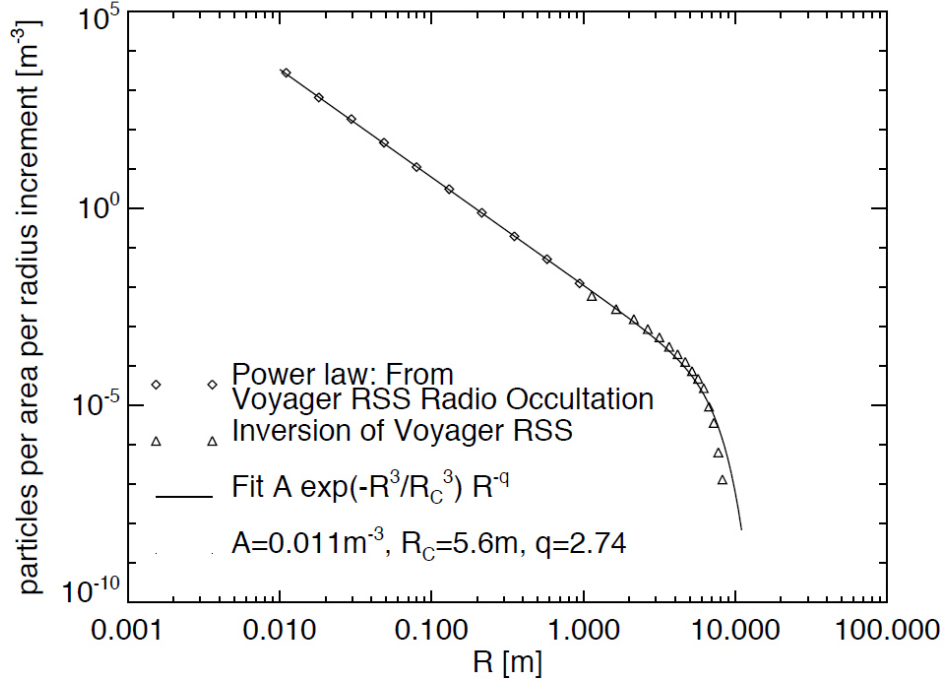


Figure 1: **Particle size distribution function.** Symbols represent the particle size distribution of Saturn's A ring inferred from data obtained by the Voyager Radio Science Subsystem (RSS) during a radio occultation of the spacecraft by the rings[2]. A fit of the theoretical curve, Eq. (4), is shown as a solid line. A cutoff radius of  $R_c = 5.6$  m, obtained from the fit, corresponds to different combinations of the primary grain size  $r_0$  and average random velocity  $\bar{V}$ . Namely, employing Eq. (4) for  $R_c$  together with  $\lambda = \left[1 - (1 + E_{\text{agg}}/\langle E \rangle)e^{-E_{\text{agg}}/\langle E \rangle}\right]^{-1} e^{-E_{\text{frag}}/\langle E \rangle}$ , one obtains a relation between  $r_0$  and  $\bar{V}$  (Supplementary Information). Solving this equation we find that  $r_0$  ranges from 4.9 cm to 2 mm, when  $\bar{V}$  varies from 0.01 cm/s to 0.1 cm/s. In particular, for  $\bar{V} = 0.03$  cm/s the primary grain size of  $r_0 = 1$  cm is obtained.



# Supplementary Online Material

## 1 Collisional mechanisms of particle aggregation and fragmentation

### 1.1 Derivation of the system of kinetic equations

In this section we derive the kinetic equations, which describe both aggregation and fragmentation of colliding particles. Here we will follow the derivation of Ref. [1] done for a similar system, but with another fragmentation model.

Consider a system comprised of particles (monomers) of mass  $m_0$  and radius  $r_0$ , which aggregate and form clusters of  $2, 3, \dots, k, \dots$  particles with masses  $m_k = km_0$ . For the purpose of kinetic description we assume here that all particles are spheres, then the characteristic radius of an agglomerate containing  $k$  monomers scales with mass as  $r_k \sim r_0 k^{1/D}$ , where  $D$  is the dimension of the aggregates. If clusters are compact,  $D = 3$ , however, the aggregates in principle can be also fractal objects with  $D < 3$ . We assume that clusters merge when the energy of the relative motion of two colliding clusters in the center-of-mass reference frame (the “relative kinetic energy” in short) is less than  $E_{\text{agg}}$ . In this case a particle of mass  $(i+j)m_0$  is formed. If the relative kinetic energy is larger than  $E_{\text{agg}}$ , but smaller than  $E_{\text{frag}}$ , the colliding particles rebound without any change of their properties. Finally, if the relative kinetic energy exceeds  $E_{\text{frag}}$ , both colliding particles disintegrate into fragments. In what follows we assume that the particles are not too large, so that the forces, which keep together particles in aggregates are of the adhesive nature, and that the gravitational interactions between the constituents may be neglected (see Sec. 1.2.1 for the detailed discussion).

Note, that recently it has been shown, that all particles with dimensions below a certain radius are absent in dense planetary rings [2]. This study justify our present model, where no particles with radii  $r < r_0$  are present in the system.

#### 1.1.1 Uniform systems

To illustrate the main ideas and to introduce the basic notations we first consider dilute and spatially uniform systems. Let  $f_i \equiv f(\vec{v}_i, t)$  be the mass-

velocity distribution function which gives the concentration of particles of mass  $m_i$  with the velocity  $\vec{v}_i$  at time  $t$ . The mass-velocity distribution function evolves according to the Boltzmann equation

$$\frac{\partial}{\partial t} f_k(\vec{v}_k, t) = I_k^{\text{agg}} + I_k^{\text{res}} + I_k^{\text{frag}} + I_k^{\text{heat}}, \quad (1)$$

where  $I_k^{\text{agg}}$ ,  $I_k^{\text{res}}$  and  $I_k^{\text{frag}}$  are, respectively, the collision integrals describing collisions leading to aggregation, restitution, and fragmentation.  $I_k^{\text{heat}}$  describes the viscous heating due to the shearing of the system in its orbital motion. The first integral reads

$$\begin{aligned} I_k^{\text{agg}}(\vec{v}_k) &= \frac{1}{2} \sum_{i+j=k} \sigma_{ij}^2 \int d\vec{v}_i \int d\vec{v}_j \int d\vec{e} \Theta(-\vec{v}_{ij} \cdot \vec{e}) |\vec{v}_{ij} \cdot \vec{e}| \times \\ &\times f_i(\vec{v}_i) f_j(\vec{v}_j) \Theta(E_{\text{agg}} - E_{ij}) \delta(m_k \vec{v}_k - m_i \vec{v}_i - m_j \vec{v}_j) \\ &- \sum_j \sigma_{kj}^2 \int d\vec{v}_j \int d\vec{e} \Theta(-\vec{v}_{kj} \cdot \vec{e}) |\vec{v}_{kj} \cdot \vec{e}| \times \\ &\times f_k(\vec{v}_k) f_j(\vec{v}_j) \Theta(E_{\text{agg}} - E_{kj}). \end{aligned} \quad (2)$$

Here  $\sigma_{ij} = r_0(i^{1/3} + j^{1/3})$  is the sum of radii of the two clusters, while  $m_k = m_i + m_j$  and  $m_k \vec{v}_k = m_i \vec{v}_i + m_j \vec{v}_j$ , due to the conservation of mass and momentum. The unit vector  $\vec{e}$  specifies the direction of the inter-center vector at the collision instant. We also introduce the reduced mass,  $\mu_{ij} = m_i m_j / (m_i + m_j)$ , the relative velocity,  $\vec{v}_{ij} = \vec{v}_i - \vec{v}_j$ , and the kinetic energy of the relative motion,  $E_{ij} = \frac{1}{2} \mu_{ij} \vec{v}_{ij}^2$ . The factors in the integrand in Eq. 2 have their usual meaning (see e.g. [3]):  $\sigma_{ij}^2 |\vec{v}_{ij} \cdot \vec{e}|$  defines the volume of the collision cylinder,  $\Theta(-\vec{v}_{ij} \cdot \vec{e})$  selects only approaching particles, while  $\Theta(E_{\text{agg}} - E_{ij})$  guarantees that the relative kinetic energy does not exceed  $E_{\text{agg}}$  to cause the aggregation. The first sum in the right-hand side of Eq. 2 refers to collisions where a cluster of mass  $k$  is formed from smaller clusters of masses  $i$  and  $j$ , while the second sum describes the collisions of  $k$ -clusters with all other aggregates.

For collisions leading to fragmentation we have

$$\begin{aligned} I_k^{\text{frag}}(\vec{v}_k) &= \frac{1}{2} \sum_i \sum_j \sigma_{ij}^2 \int d\vec{v}_j \int d\vec{v}_i \int d\vec{e} \Theta(-\vec{v}_{ij} \cdot \vec{e}) |\vec{v}_{ij} \cdot \vec{e}| f_j(\vec{v}_j) f_i(\vec{v}_i) \times \\ &\times \Theta(E_{ij}^n - E_{\text{frag}}) (q_{ki}(\vec{v}_k, \vec{v}_i, \vec{v}_j) + q_{kj}(\vec{v}_k, \vec{v}_i, \vec{v}_j)) \\ &- \sum_i (1 - \delta_{k,1}) \sigma_{ki}^2 \int d\vec{v}_i \int d\vec{e} \Theta(-\vec{v}_{ki} \cdot \vec{e}) |\vec{v}_{ki} \cdot \vec{e}| \times \end{aligned} \quad (3)$$

$$\times f_k(\vec{v}_k) f_i(\vec{v}_i) \Theta(E_{ki}^n - E_{\text{frag}}) ,$$

where we define the kinetic energy of the relative *normal* motion,  $E_{ij}^n = \frac{1}{2}\mu_{ij}(\vec{v}_{ij} \cdot \vec{e})^2$ , with  $(\vec{v}_{ij} \cdot \vec{e})$  being the normal relative velocity. Note that in contrast to the case of aggregation, where both normal and tangential components must be small, so that the total energy of the relative motion  $E_{ij}$  matters, for a fragmentation process only the relative normal motion is important: It causes a compression and the subsequent breakage of particles' material. Hence the kinetic energy of the relative *normal* motion,  $E_{ij}^n$  must exceed some threshold. The first sum in Eq. 3 describes the collision of particles  $i$  and  $j$  with the relative kinetic energy of the normal motion above the fragmentation threshold  $E_{\text{frag}}$  and  $q_{ki}(\vec{v}_k, \vec{v}_i, \vec{v}_j)$  gives the number of debris of mass  $m_k = m_0 k$  with the velocity  $\vec{v}_k$ , when a particle of mass  $m_i = m_0 i$  desintegrates at a collision with a particle of mass  $m_j = m_0 j$ , provided that the according pre-collision velocities are  $\vec{v}_i$  and  $\vec{v}_j$ . Obviously,  $q_{ki} = 0$  if  $k \geq i$ . The function  $q_{ki}(\vec{v}_k, \vec{v}_i, \vec{v}_j)$  depends on the particular collision model. For the purpose of the present study we restrict the analytical model on the case of complete disruption of clusters into monomers (section 2). However, numerical results for more general cases, when particles decay in debris with a power-law size distribution, are also shown for comparison in section 2.2. The second sum describes the process, when particles of mass  $k \neq 1$  break in collisions with all other particles. The collision integral for the restitutive collisions has its usual form [3],

$$\begin{aligned} I_k^{\text{res}}(\vec{v}_k) &= \sum_i \sigma_{ki}^2 \int d\vec{v}_i \int d\vec{e} \Theta(-\vec{v}_{ki} \cdot \vec{e}) |\vec{v}_{ki} \cdot \vec{e}| \times \\ &\times \left( \varepsilon_{ki}^{-2} f_k(\vec{v}_k'') f_i(\vec{v}_i'') - f_k(\vec{v}_k) f_i(\vec{v}_i) \right) \Theta(E_{ki} - E_{\text{agg}}) \Theta(E_{\text{frag}} - E_{ki}) , \end{aligned} \quad (4)$$

with a slight modification to account the requirements for the relative kinetic energy:  $E_{ij} > E_{\text{agg}}$  and  $E_{ij}^n < E_{\text{frag}}$ . Here  $\vec{v}_k''$  and  $\vec{v}_i''$  are the initial velocities for the so-called inverse collision, which results with the velocities  $\vec{v}_k$  and  $\vec{v}_i$ , and  $\varepsilon_{ki}$  is the restitution coefficient for a collision between particles of size  $k$  and  $i$ , e.g. [3].

For the heating term we adopt the following simple model, e.g. [4]

$$I_k^{\text{heat}} = \frac{\Gamma_k}{2} \frac{\partial^2}{\partial \vec{v}_k^2} f_k(\vec{v}_k, t) , \quad (5)$$

where  $\Gamma_k$  is the rate of heating of the species with mass  $m_k$ .

Owing to the permanent aggregation and fragmentation we have a dynamically sustained mixture of particles of different mass. Mixtures of dissipative particles, generally, have different velocity dispersion, or mean kinetic energy ("granular temperature") of each species. We define the partial number density  $n_i$  and mean kinetic energy  $\langle E_i \rangle$  of the species as [5],

$$n_i = \int d\vec{v}_i f_i(\vec{v}_i), \quad \frac{3}{2}n_i\langle E_i \rangle = \int \frac{1}{2}m_i\vec{v}_i^2 f(m_i, \vec{v}_i) d\vec{v}_i, \quad (6)$$

We assume that the distribution function  $f_i(\vec{v}_i, t)$  may be written as [6, 7, 5]

$$f_i(\vec{v}_i, t) = \frac{n_i(t)}{v_{0,i}^3(t)} \phi_i(\vec{c}_i), \quad \vec{c}_i \equiv \frac{\vec{v}_i}{v_{0,i}}, \quad (7)$$

where  $v_{0,i}^2(t) = 2\langle E_i \rangle(t)/m_i$  is the thermal velocity and  $\phi(c_i)$  the reduced distribution function. For the force-free granular mixtures the velocity distribution functions of the components are not far from the Maxwellian distribution [5], which reads in terms of the reduced velocity  $\vec{c} = \vec{v}/v_0$ ,

$$\phi_M(\vec{c}) = \pi^{-3/2} \exp(-c^2). \quad (8)$$

The equipartition between different components, however, breaks down in general for granular systems, in the sense that the average kinetic energies for each size group  $\langle E_i \rangle$  are not equal [5].

Integrating Eq. 1 over  $\vec{v}_k$  we obtain the equations for the zero-order moments of the velocity distribution functions  $f_k$ , that is, for the concentrations  $n_k$ . Taking into account that collisions resulting in rebounds do not change the concentrations of different species and using Eqs. 2–3 together with Eqs. 6–8 we arrive at the rate equations

$$\begin{aligned} \frac{d}{dt}n_k &= \frac{1}{2} \sum_{i+j=k} C_{ij}n_in_j - n_k \sum_i C_{ki}n_i - \sum_i A_{ki}n_kn_i(1 - \delta_{k1}) \\ &+ \frac{1}{2} \sum_{i,j} A_{ij}n_in_j (x_k(i) + x_k(j)), \end{aligned} \quad (9)$$

where  $x_k(i)$  is the total number of debris of size  $k$ , produced in the disruption of a particle of size  $i$ .<sup>1</sup> Note that  $x_k(i) = 0$  if  $k \geq i$  and  $\sum_k kx_k(i) = i$ . In

---

<sup>1</sup> The value of  $x_k(i)$  may be expressed in terms of  $Q_{k,i,j}(z) = Q_{k,i,j}((\vec{v}_{ij} \cdot \vec{e})^2) = \int q_{ki}(\vec{v}_k, \vec{v}_i, \vec{v}_j) d\vec{v}_k$ , where we assume that the disruption outcome depends only on the square of relative normal velocity  $z = (\vec{v}_{ij} \cdot \vec{e})^2$  as  $x_k(i) = x_k(i, j) = \frac{1}{2}\mu_{ij}B_{ij}e^{B_{ij}E_{\text{frag}}} \int_0^\infty e^{-\frac{1}{2}\mu_{ij}B_{ij}z} Q_{k,i,j}(z) \Theta(z - 2E_{\text{frag}}/\mu_{ij}) dz$ .

what follows we will use the model expressions for the coefficients  $x_k(i)$ , like  $x_k(i) = i\delta_{1k}$ , or  $x_k(i) \sim k^{-\alpha}$ , which do not depend on the velocity dispersion or aggregation and fragmentation energies.

The rate coefficients  $C_{ij}$  and  $A_{ij}$  in the above equation read:

$$\begin{aligned}
C_{ij} &= \nu_{ij} \lambda_{\text{agg}} \\
A_{ij} &= \nu_{ij} \lambda_{\text{frag}} \\
\nu_{ij} &= 2\sigma_{ij}^2 \sqrt{2\pi \left( \frac{\langle E_i \rangle}{m_i} + \frac{\langle E_j \rangle}{m_j} \right)} \\
\lambda_{\text{agg}} &= 1 - (1 + B_{ij} E_{\text{agg}}) \exp(-B_{ij} E_{\text{agg}}) \\
\lambda_{\text{frag}} &= \exp(-B_{ij} E_{\text{frag}}) \\
B_{ij} &= \frac{m_i + m_j}{\langle E_i \rangle m_j + \langle E_j \rangle m_i}.
\end{aligned} \tag{10}$$

Here  $\nu_{ij}n_in_j$  give the collision frequency between particles of size  $i$  and  $j$  and  $\lambda_{\text{agg}}$  and  $\lambda_{\text{frag}}$  give respectively the fraction of aggregative and disruptive collisions. It is useful to verify that the above kinetic equation (9) fulfills the condition of mass conservation,  $\sum_k km_0 n_k = M = \text{const.}$ , where  $M$  is the total mass density.

If  $E_{\text{frag}} = \text{const.}$ ,  $E_{\text{agg}} = \text{const.}$  and  $\langle E_i \rangle = \langle E \rangle \equiv E_{\text{av}}$ , the rate coefficients  $A_{ij}$  and  $C_{ij}$  are proportional and differ only by the multiplicative constant  $\lambda = \lambda_{\text{frag}}/\lambda_{\text{agg}}$ :

$$\begin{aligned}
C_{ij} &= 2\sigma_{ij}^2 \sqrt{2\pi E_{\text{av}}(m_i^{-1} + m_j^{-1})} \left[ 1 - (1 + E_{\text{agg}}/E_{\text{av}}) e^{-E_{\text{agg}}/E_{\text{av}}} \right] \\
A_{ij} &= \lambda C_{ij}, \quad \lambda = \left[ 1 - (1 + E_{\text{agg}}/E_{\text{av}}) e^{-E_{\text{agg}}/E_{\text{av}}} \right]^{-1} e^{-E_{\text{frag}}/E_{\text{av}}}.
\end{aligned} \tag{11}$$

In what follows we assume for simplicity that the above form of the kinetic coefficients holds generally, that is, the dependence of the rate kernel on the particles size occurs only through the collision frequency  $\nu_{ij}$

$$\begin{aligned}
C_{ij} &= \text{const.} \times \nu_{ij} \\
A_{ij} &= \lambda C_{ij},
\end{aligned} \tag{12}$$

where  $\lambda$  is a constant.

### 1.1.2 Self-gravity wakes and ring structure

Saturn's rings are not uniform but exhibit a large variety of structures [8]. One example are the self-gravity wakes [9, 10, 11, 12], arising from self-

gravitational instability, forming a transient and fluctuating pattern in the surface mass density of the rings, canted relative to the azimuthal direction, with a typical length scale of about  $L_w \sim 10^2$  m, one Toomre critical wavelength [13]. Thus, to describe adequately particle kinetics one needs in principle to take into account effects of dense packing, non-homogeneity, and gravitational interactions between particles. Two important comments are to be done in this respect. First, due to the low velocity dispersion of particles in the dense parts of the wakes, the collision duration is still significantly smaller than the time between particle collisions. This implies the validity of the assumption of binary collisions, as the dominant mechanism of particles' kinetics. For the same reason, the the method of molecular dynamics simulations, based on the binary collision hypothesis, is applicable to study the dynamics of dense rings [14]. Therefore a kinetic description in terms of the Enskog-Boltzmann equation is possible [15]. Although this Markovian equation ignores memory effects in particle kinetics, it may be still applicable, when the mean free path is comparable to, or even smaller than the particle size [16]. Second, the characteristic length scale of the density wakes,  $L_w$ , and the upper cut-off radius (about  $10m$ ) are well separated. This allows to neglect variations of density and distribution functions on the latter length scale and use a local approximation for the distribution function of two particles at contact:

$$f_2(\vec{v}_k, \vec{r} - \vec{e}r_k, \vec{v}_l, \vec{r} + \vec{e}r_l, t) \simeq g_2(\sigma_{lk})f_k(\vec{v}_k, \vec{r}, t)f_l(\vec{v}_l, \vec{r}, t) \quad (13)$$

where  $f_2$  is the two-particle distribution function, for particles of radius  $r_k$ , and  $r_l$ , which have a contact at point  $\vec{r}$ , the unit vector  $\vec{e}$  joins the centers of particles and  $g_2(\sigma_{lk})$  is the contact value of the pair distribution function, which may be well approximated by its equilibrium value for the hard sphere fluid; explicit expressions for  $g_2(\sigma_{lk})$  may be found, e.g. in [3]. In the local approximation (Eq. 13) the collision integrals depend only on local values at a particular space point  $\vec{r}$ . This significantly simplifies the kinetic description of a high-density gas, since the density effects are taken into account in this approach by the multiplicative Enskog factor,  $g_2(\sigma_{lk})$ , leaving the structure of the collision integrals unchanged. Therefore the Enskog-Boltzmann equation valid for the case of wakes reads:

$$\begin{aligned} \frac{\partial}{\partial t} f_k(\vec{v}_k, \vec{r}, t) + \vec{v}_k \cdot \vec{\nabla} f_k(\vec{v}_k, \vec{r}, t) + \vec{F}_k(\vec{r}) \cdot \frac{\partial}{\partial \vec{v}_k} f_k(\vec{v}_k, \vec{r}, t) = \\ = I_k^{\text{agg}}(\vec{r}) + I_k^{\text{res}}(\vec{r}) + I_k^{\text{frag}}(\vec{r}), \end{aligned} \quad (14)$$

where  $f_k(\vec{v}_k, \vec{r}, t)$  is the velocity distribution function of particles of size  $k$  (comprised of  $k$ -monomers), which depends on the space coordinate  $\vec{r}$  and  $\vec{F}_k(\vec{r})$  is the total gravitational force, acting on the particle of size  $k$ , which includes both the gravitational force from the central planet as well as self-gravitation of the ring particles. In what follows we do not need an explicit expression for this term. The collision integrals in the r.h.s. of Eq. 14 have the same form as in the previous case of a uniform system, with the only difference, that they depend on local parameters taken at a point  $\vec{r}$ , and that the collision cross-sections are re-normalized according to the rule:

$$\sigma_{ij}^2 \longrightarrow \sigma_{ij}^2 g_2(\sigma_{ij}) \quad (15)$$

which accounts for the high-density effects in the local approximation, see e.g. [3]. Note that we do not need here the term  $I_k^{\text{heat}}(\vec{r})$ , which mimicked heating for the model of a uniform gas, since the Eq. 14 implicitly contains the spacial gradients and fluxes, responsible for the heating.

If we now integrate (as in the case of a uniform gas) the kinetic equation 14 over  $\vec{v}_k$ , we find the equations for the concentrations  $n_k(\vec{r})$ :

$$\begin{aligned} \frac{\partial}{\partial t} n_k(\vec{r}) + \vec{\nabla} \cdot \vec{j}_k(\vec{r}) = & \frac{1}{2} \sum_{i+j=k} C_{ij}(\vec{r}) n_i(\vec{r}) n_j(\vec{r}) - n_k(\vec{r}) \sum_i C_{ki}(\vec{r}) n_i(\vec{r}) \\ & + \sum_i A_{ki}(\vec{r}) n_k(\vec{r}) n_i(\vec{r}) (1 - \delta_{k1}) + \frac{1}{2} \sum_{i,j} A_{ij}(\vec{r}) n_i(\vec{r}) n_j(\vec{r}) (x_k(i) + x_k(j)) , \end{aligned} \quad (16)$$

where the partial flux  $\vec{j}_k(\vec{r})$  is defined as

$$\vec{j}_k(\vec{r}) = \int \vec{v}_k f_k(\vec{v}_k, \vec{r}, t) d\vec{v}_k .$$

It describes the macroscopic (hydrodynamic flux), associated with particles of size  $k$ . The important difference of Eq. 16 from Eq. 9, used for a uniform system, is the spatial dependence of the kinetic coefficients  $A_{ij}$  and  $C_{ij}$ . Although the structure of these coefficients coincides with that of Eqs.10 (apart from the trivial re-normalization, Eq. 15), all quantities here are local. Naturally, the local velocity dispersion  $\langle E_i \rangle(\vec{r})$  in the dense parts of the wakes significantly differs from that of the dilute regions inbetween.

Now we average Eqs. 16 over a suitable control volume  $V$ , which contains a large number of wakes. Applying then Green's theorem and taking into

account that the surface integral of the flux  $\vec{j}_k$  over the boundary of the control volume vanishes as  $1/V$ ,

$$\int \vec{\nabla} \cdot \vec{j}_k d\vec{r} = \int_S \vec{j}_k \cdot d\vec{s} = 0,$$

we finally arrive at a set of equations of the same form as Eqs. 9, but with the space-averaged quantities:

$$\begin{aligned} \frac{d}{dt} \bar{n}_k &= \frac{1}{2} \sum_{i+j=k} \bar{C}_{ij} \bar{n}_i \bar{n}_j - \bar{n}_k \sum_i \bar{C}_{ki} \bar{n}_i - \sum_i \bar{A}_{ki} \bar{n}_k \bar{n}_i (1 - \delta_{k1}) \\ &+ \frac{1}{2} \sum_{i,j} \bar{A}_{ij} \bar{n}_i \bar{n}_j (x_k(i) + x_k(j)). \end{aligned} \quad (17)$$

Here, by the definition,

$$\bar{n}_k = \frac{1}{V} \int n_k(\vec{r}) d\vec{r}.$$

and

$$\bar{C}_{ij} = \frac{1}{\bar{n}_i \bar{n}_j} \frac{1}{V} \int n_i(\vec{r}) n_j(\vec{r}) C_{ij}(\vec{r}) d\vec{r},$$

where  $C_{ij}(\vec{r})$  are defined by Eqs. 10 with the local velocity dispersions  $\langle E_i \rangle(\vec{r})$ . Similar expression holds true for the coefficients  $\bar{A}_{ij}$ .

It is important to note that the coefficients  $\bar{C}_{ij}$  and  $\bar{A}_{ij}$  are density-weighted quantities. Therefore the contribution to the average value is proportional to the local density. This in turn implies that the values of these coefficients practically coincide with these for the dense part of the wakes,

$$\bar{C}_{ij} = C_{ij}^{(dense\ part)} \quad \bar{A}_{ij} = A_{ij}^{(dense\ part)}.$$

Hence we conclude that the kinetic equations for the average concentrations of particles  $\bar{n}_k$  coincide with the previously derived equations for  $n_k$  for the case of a uniform system. In what follows we will use  $n_k$ ,  $C_{ij}$  and  $A_{ij}$  for the notation brevity, keeping although in mind that they correspond to the average values, that are almost equal to these values in the dense part of the wakes.



## 1.2 Tidal forces and gravitational versus adhesive energy of aggregates

### 1.2.1 Impact of the tidal forces on the aggregate disruption

In the previous section we considered only the collisional mechanism of aggregates disruption. The rings particles, however, also suffer from tidal forces and we wish to estimate the impact of these forces on the aggregates stability. If the critical stress of the material of a body subjected to tidal forces is  $P_{\max}$ , the condition of the tidal disruption reads [17],

$$P_{\max} < 1.68 \rho_b R_b^2 \Omega^2 \quad (18)$$

where  $\rho_b$  is the density of the body,  $R_b$  its radius and  $\Omega$  is the Kepler frequency. For solid ice the above equation yields 200 km for the critical radius of tidal disruption. In application to aggregates of radius  $R$  comprised of spherical ice particles of radius  $r_0$ , we can estimate the critical pressure and critical radius as follows. The area of the equatorial aggregate cross-section  $\pi R^2$  contains  $\phi \pi R^2 / \pi r_0^2 = \phi (R/r_0)^2$  particles' contacts, where  $\phi$  is the mean packing fraction of the aggregate composed of primary grains. All primary particles are kept in the aggregate by the adhesive forces. According to the JKR theory [18] the maximal pulling force which an adhesive contact can resist, reads,

$$f_0 = \frac{3}{2} \pi \gamma \frac{r_0}{2} \quad (19)$$

where  $\gamma$  is the surface tension of the particle material. The total force which can resist a body with the cross-section  $\pi R^2$  is  $\phi (R/r_0)^2 f_0$ , hence the maximal resistance to pulling may be estimated as

$$P_{\max} = \frac{3}{4} \phi \frac{\gamma}{r_0} \quad (20)$$

Using  $r_0 = 1 \text{ cm}$ ,  $\gamma = 0.74 \text{ N/m}$  and  $\phi = 0.4$ , we obtain  $P_{\max} = 22.2 \text{ N/m}^2$ . With the density of the aggregates of  $\phi \rho_{\text{ice}} = 400 \text{ kg/m}^3$  and  $\Omega = 1.5 \cdot 10^{-4} \text{ s}^{-1}$  we obtain the disruption radius of  $1.211 \cdot 10^3 \text{ m} = 1.2 \text{ km}$ . If we assume that the primary grain size is ten times bigger,  $r_0 = 10 \text{ cm}$ , and the surface tension is 10 times smaller, due to the surface roughness of the particles,  $\gamma = 0.074 \text{ N/m}$ , we still obtain the disruption radius of  $121 \text{ m}$ , which is one order of magnitude larger than the cutoff radius  $R_c$ , observed for the particle size distribution in the Rings. Hence we conclude that the disruption of particles due to the tidal forces may be safely neglected.

### 1.2.2 Gravitational versus adhesive energy of aggregates

In our study we concentrate on the aggregates, comprised of particles kept by adhesive forces. It is instructive to compare the total energy of all adhesive bonds with the gravitational energy of aggregates (for detailed discussion of this issue see the forthcoming article [19]). The total gravitational energy reads,

$$E_G = \frac{G}{2} \sum_{i=1}^N \sum_{j=1, j \neq i}^N \frac{m_i m_j}{|\vec{r}_i - \vec{r}_j|} \simeq \frac{G}{2} \int d\vec{r}_1 \int d\vec{r}_2 \frac{\rho(\vec{r}_1) \rho(\vec{r}_2)}{|\vec{r}_1 - \vec{r}_2|} = \frac{3GM^2}{5R},$$

where  $G$  is the gravitational constant and we approximate the discrete distribution of  $N$  particles of mass  $m_i$  at spatial points  $\vec{r}_i$  by the continuum uniform mass distribution with density  $\rho(\vec{r}) = \rho_{\text{ice}}\phi$ ; here  $\rho_{\text{ice}} \simeq 10^3 \text{ kg/m}^3$  is the density of the constituents (ice particles) and  $\phi \approx 0.4$  is the average packing fraction of the aggregate. The total mass of the aggregate of radius  $R$  then reads,

$$M = \sum_{i=1}^N m_i = \frac{4}{3}\pi R^3 \rho_{\text{ice}} \phi.$$

This gives for the gravitational energy in the SI units:

$$E_G = 1.124 \cdot 10^{-5} R^5 [J].$$

The total adhesive energy, equal to the energy of all adhesive bonds in aggregate of radius  $R$ , comprised of spheres of radius  $r_0$ , is computed below in section 4. The result reads in SI units (this energy is termed as "average fragmentation energy" below)

$$E_{\text{adh}} = 8.2 \cdot 10^{-7} R^3 r_0^{-5/3} [J]$$

For the typical values of  $R \sim 1\text{m}$  and  $2r_0 \sim 0.01\text{m}$ , the adhesive energy is almost two order of magnitude larger than the gravitational energy. For larger radii  $R$ , close to the cut-off values,  $R \approx 5\text{m}$ , the adhesive energy is still few times larger than the gravitational one.

These estimates motivate our approximate treatment of the aggregates: With an acceptable accuracy, we will neglect the gravitational interactions of particles in the aggregates and take into account only the adhesive interactions.

## 2 Solution of the rate equations

### 2.1 Analytical approach

We start the analysis from the simplest fragmentation model – the complete fragmentation into monomers of both colliding particles; in this case  $x_k(i) = i\delta_{1k}$ . We also assume that the mean kinetic energy is the same for all species, so that  $A_{ij} = \lambda C_{ij}$ . In this case the rate equations take the simplified form,

$$\frac{dn_k}{dt} = \frac{1}{2} \sum_{i+j=k} C_{ij} n_i n_j - (1 + \lambda) n_k \sum_{j \geq 1} C_{kj} n_j \quad (21)$$

for evolution of clusters of mass  $k > 1$ . The parameter  $\lambda$ , given by equation (11), characterizes the relative weight of fragmentation. The governing equation for the monomer density reads

$$\frac{dn_1}{dt} = -n_1 \sum_{j \geq 1} C_{1j} n_j + \frac{\lambda}{2} \sum_{i,j \geq 2} C_{ij} (i + j) n_i n_j + \lambda n_1 \sum_{j \geq 2} j C_{1j} n_j \quad (22)$$

Similar equations with terms responsible for the spontaneous fragmentation of aggregates have been analyzed in Ref. [20, 21] in the context of rain drop formation.

#### 2.1.1 Constant kernel

*Evolution kinetics.* Consider first a model with mass-independent kernel  $C_{ij} = C_0$ . For this kernel, Eqs. 21–22 simplify to

$$\frac{dn_k}{dt} = \frac{1}{2} \sum_{i+j=k} n_i n_j - (1 + \lambda) n_k N \quad (23)$$

and

$$\frac{dn_1}{dt} = -n_1 N + \lambda(1 - n_1) N. \quad (24)$$

where we re-scale time  $t \rightarrow C_0 n_0 t$  and densities  $n_k \rightarrow n_0 n_k$ , leaving for the re-scaled quantities the old notations. Here

$$N(t) = \sum_{j \geq 1} n_j(t) \quad (25)$$

is the total cluster density.  $n_0$  in the last equations (23)–(25) is the characteristic concentration of particles, say the concentration of monomers, and  $C_0$  is

the characteristic value of the (equal) rate coefficients  $C_{ij}$ , so that  $C_0 n_0$  gives the characteristic frequency of aggregative collisions. Summing all equations (23) and equation (24) we arrive at a closed equation for the cluster density:

$$\frac{dN}{dt} = -N^2 + 2\lambda(1 - N)N \quad (26)$$

Consider for concreteness the mono-disperse initial condition  $n_k(t = 0) = \delta_{k,1}$ . Solving (26) subject to  $N(0) = 1$  gives

$$N(t) = \frac{2\lambda}{1 + 2\lambda - e^{-2\lambda t}}. \quad (27)$$

Plugging this into (24) and solving subject to  $n_1(0) = 1$  we obtain  $n_1(t)$ :

$$n_1(t) = \frac{\lambda}{1 + \lambda} + \frac{1}{1 + \lambda} \Lambda(t) \quad \text{with} \quad \Lambda(t) = \left[ \frac{(1 + 2\lambda)e^{2\lambda t} - 1}{2\lambda} \right]^{-\frac{2(1+\lambda)}{1+2\lambda}} \quad (28)$$

and then, recursively, from equation (23) all  $n_k(t)$  with  $k > 1$ . These relations, however, quickly get very unwieldy as the mass  $k$  grows and we do not present them here. The straightforward analysis shows that the system reaches a non-trivial steady state,  $n_k(t) \rightarrow n_k$  and the characteristic relaxation time is essentially the relaxation time for the total density of clusters  $N(t)$ . From Eq. 27 follows the dimensionless relaxation time,  $\tau_{\text{rel}}^{-1} = 2\lambda$ ; therefore, from Eq. 11 we obtain the dimensional relaxation time

$$\tau_{\text{rel}}^{-1} \sim C_0 n_0 \lambda \sim R_{\text{av}}^2 \bar{V} n_0 e^{-E_{\text{frag}}/E_{\text{av}}},$$

which actually coincides with the average collision time for disruptive collisions. Here  $R_{\text{av}}$  is the characteristic size of particles and  $\bar{V}$  is their mean random velocity. With the mean packing fraction  $\nu_0 = (4\pi/3)R_{\text{av}}^3 n_0$  for the ring particles, the last equation takes the form,

$$\tau_{\text{rel}}^{-1} \sim \bar{V} \nu_0 R_{\text{av}}^{-1} e^{-E_{\text{frag}}/E_{\text{av}}} \quad (29)$$

Using  $\bar{V} = 10^{-4} - 10^{-3}$  m/s, the average particle size  $R_{\text{av}} \sim 1$  m, the packing fraction  $\nu_0 = 10^{-2} - 10^{-1}$  and the exponential factor, estimated for this random velocity interval, as  $4 \times 10^{-14} - 3 \times 10^{-7}$  (see Section 4), we obtain as a lower boundary for relaxation time of the system,

$$\tau_{\text{rel}} > 1,000 \text{ years}.$$

This is the characteristic time for the rings to return from a perturbed state to their proper steady-state size distribution.

*Steady-state size distribution.* To obtain the steady-state solution we write the governing equations

$$0 = \sum_{i+j=k} n_i n_j - (1 + \lambda) n_k N \quad (30)$$

which suggests to use the generating function technique. Multiplying (30) by  $z^k$  and summing over  $k = 2, 3, \dots$  we obtain a simple quadratic equation

$$\mathcal{N}(z)^2 - 2(1 + \lambda) N \mathcal{N}(z) + 2(1 + \lambda) N n_1 z = 0 \quad (31)$$

for the generating function

$$\mathcal{N}(z) = \sum_{k \geq 1} n_k z^k \quad (32)$$

Solving (31) yields

$$\mathcal{N}(z) = (1 + \lambda) N \left[ 1 - \sqrt{1 - \frac{2n_1}{(1 + \lambda)N} z} \right] \quad (33)$$

Expanding  $\mathcal{N}(z)$  we arrive at

$$n_k = \frac{N}{\sqrt{4\pi}} (1 + \lambda) \left[ \frac{2n_1}{(1 + \lambda)N} \right]^k \frac{\Gamma(k - \frac{1}{2})}{\Gamma(k + 1)} \quad (34)$$

Using the already known expressions (27, 28) for the (steady state) densities of the monomers and the total number of clusters

$$n_1 = \frac{\lambda}{1 + \lambda}, \quad N = \frac{2\lambda}{1 + 2\lambda} \quad (35)$$

we recast (34) into the form

$$n_k = A a^k \frac{\Gamma(k - \frac{1}{2})}{\Gamma(k + 1)} \quad (36)$$

where

$$A = \frac{1}{4\sqrt{\pi}} \frac{\lambda(1 + \lambda)}{1 + 2\lambda}, \quad a(\lambda) = 1 - \left( \frac{\lambda}{1 + \lambda} \right)^2 \quad (37)$$

When  $\lambda \ll 1$ , equation (36) becomes

$$n_k = \frac{\lambda}{\sqrt{\pi}} e^{-\lambda^2 k} \frac{\Gamma(k - \frac{1}{2})}{\Gamma(k + 1)} \quad (38)$$

which can be further simplified to

$$n_k = \frac{\lambda}{\sqrt{\pi}} e^{-\lambda^2 k} k^{-3/2} \quad (39)$$

when  $k \gg 1$ . Thus in the region  $k < \lambda^{-2}$ , the mass distribution exhibits a power-law dependence with an exponential cutoff for larger  $k$ .

### 2.1.2 Generalized Product Kernels

*Equal mean energy.* We again assume that  $E_{\text{frag}} = \text{const.}$ ,  $E_{\text{agg}} = \text{const.}$  and that all species have the same mean energy  $E_{\text{av}}$ . Then the rate constants read,

$$C_{ij} = C_0 (i^{1/3} + j^{1/3})^2 (i^{-1} + j^{-1})^{1/2}, \quad A_{ij} = \lambda C_{ij} \quad (40)$$

where the constants  $C_0$  and  $\lambda$  are determined by Eqs. 11.

It seems impossible to solve (21) for the rate coefficients (40); even in the steady state, the equations appear intractable. An old trick in the field of aggregation is to replace the kernel by a simpler one with the same degree of homogeneity. The reason is that the homogeneity degree is often the only characteristics that affects the behavior. Therefore one can use the generalized product kernel

$$K_{ij} = (ij)^\mu \quad (41)$$

with the same degree of the homogeneity

$$2\mu = 2/3 - 1/2 = 1/6, \quad \text{or} \quad \mu = 1/12$$

which is analytically solvable. Indeed, the governing equations in this case become (we again use the re-scaled densities  $n_k \rightarrow n_0 n_k$ ),

$$0 = \sum_{i+j=k} l_i l_j - (1 + \lambda) l_k M \quad (42)$$

in the steady state. Here we have used the notation

$$l_k = k^\mu n_k, \quad M = \sum_{k \geq 1} l_k \quad (43)$$

Equation (42) are mathematically identical to Eqs. 30 and therefore they admit the same solution (recall that  $l_1 = n_1$ )

$$\mathcal{M}(z) = (1 + \lambda) M \left[ 1 - \sqrt{1 - \frac{2n_1}{(1 + \lambda)M} z} \right] \quad (44)$$

where  $\mathcal{M}(z)$  is the generating function

$$\mathcal{M}(z) = \sum_{k \geq 1} l_k z^k \quad (45)$$

Therefore the solution reads

$$n_k = \frac{M}{\sqrt{4\pi}} (1 + \lambda) \left[ \frac{2n_1}{(1 + \lambda)M} \right]^k \frac{\Gamma(k - \frac{1}{2})}{k^\mu \cdot \Gamma(k + 1)} \quad (46)$$

The analysis shows that  $2n_1/[(1 + \lambda)M] = a$  with  $a$  given by (37) does not depend on  $\mu$ . Thus the solution (46) can be re-written as

$$n_k = \frac{(1 + \lambda)M}{2\sqrt{\pi}} a^k \frac{\Gamma(k - \frac{1}{2})}{k^\mu \cdot \Gamma(k + 1)} \quad (47)$$

The quantity  $M$  can in principle be found from the sum rule and the behavior again simplifies in the small  $\lambda$  limit. Asymptotically (when  $1 \ll k < \lambda^{-2}$ ) we get

$$n_k = \frac{M}{2\sqrt{\pi}} e^{-\lambda^2 k} k^{-3/2-\mu} \quad (48)$$

which is again the power-law behavior with the exponential cutoff. Note that the scaling,  $n_k \sim k^{-3/2-\mu}$  has been obtained previously in Ref. [21].

*Equal mean dispersion velocity.* If we now assume that all ring particles have the same mean velocity dispersion,  $\langle V^2 \rangle = \langle V_i^2 \rangle$ , that is  $\langle E_i \rangle = m_i \langle V^2 \rangle$ , Eqs. 10 give

$$C_{ij} = C_0 \left( i^{1/3} + j^{1/3} \right)^2, \quad A_{ij} = \lambda C_{ij}, \quad (49)$$

with the homogeneity degree

$$2\mu = 2/3, \quad \text{or} \quad \mu = 1/3,$$

different from that obtained for the model of equal mean kinetic energy of rings particles. Note that the model of equal velocity dispersion implies

that  $\langle E_i \rangle \sim i$ , while for the model of equal mean energy  $\langle E_i \rangle \sim i^0$ . For the former case  $\mu = 1/12$ , and for the latter  $\mu = 1/3$ . Physically, one expects that the energy of ring particles obeys the relation,  $\langle E_i \rangle \sim i^\gamma$ , where  $0 \leq \gamma \leq 1$ . Indeed,  $\gamma$  can not be negative, since this would imply that very big particles do not have velocity dispersion, which is only possible for unrealistic condition of the collision-free motion. At the same time the condition  $\gamma > 1$  is also not realistic, since it would imply that the energy, pumped in due to collisions, increases with particle mass faster than linearly; obviously, there is no evidence of such processes. Hence we conclude that  $\gamma$  is limited within the interval  $[0, 1]$ , and, correspondingly,  $\mu$  obeys the restrictions  $1/12 \leq \mu \leq 1/3$ .

## 2.2 Numerical analysis of the rate equations

To verify the validity of various approximations made in the analytical solution resented in the previous section we additionally perform a numerical analysis. We explicitly solve the system of rate equations. First, we observe that the exact rate coefficients and the rate coefficients for the product kernel with the same degree of homogeneity indeed give practically identical results, (Fig. 1). We also compare the fragmentation model with complete breakage (studied in the previous section) to a model with power law distributed debris sizes ( $x_k(i) \sim k^{-\alpha}$ ). The results are shown in Fig. 2. As one can see from the figure the both models (of the complete disruption and of the breakage with the power-law distribution of debris size) develop practically the same slope if the distribution of debris size in a collision is steep enough,  $\alpha \geq 2$ . The steep distribution implies strong domination of small fragments, which seems very plausible from the physical point of view: Indeed, the aggregates are relatively loose objects, with the small average coordination number. For such object it would be much easier to create small debris in a fragmentation process, as compared to the case of large coordination number.

## 3 Size Distribution

In observations the size distribution of particles can be constrained. Using the relation  $k \sim R^3$  (for spherical particles) in conjunction with  $n_k dk = f(R) dR$  we find that  $n_k \sim k^{-3/2-\mu}$  implies

$$f(R) \sim R^{-q} e^{-(R/R_c)^3} \quad q = 5/2 + 3\mu \quad R_c^3 = 4r_0^3/\lambda^2 \quad (50)$$



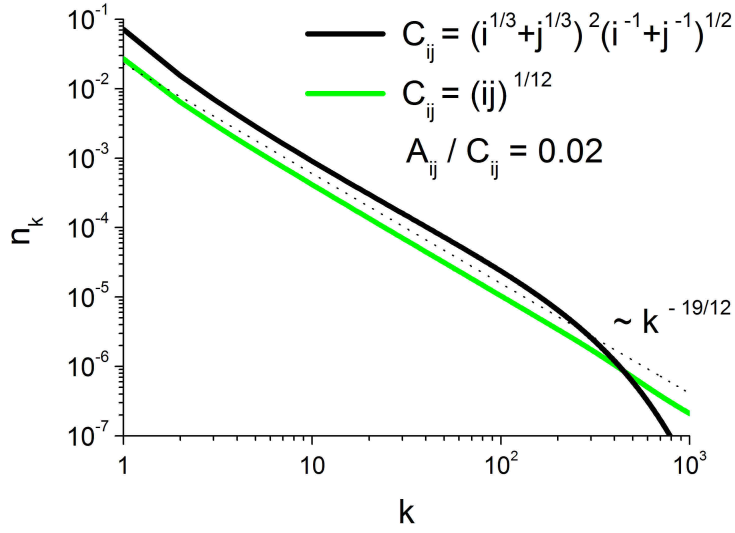


Figure 1: Size distribution from the model given by equations (21, 22) for two different kernels with the same degree of homogeneity – the ballistic kernel and the simplified product kernel. The slope of the power law regime of the theoretical prediction,  $n_k \propto k^{19/12}$ , is shown as a dotted line. The fragmentation parameter is  $\lambda = 0.02$ .

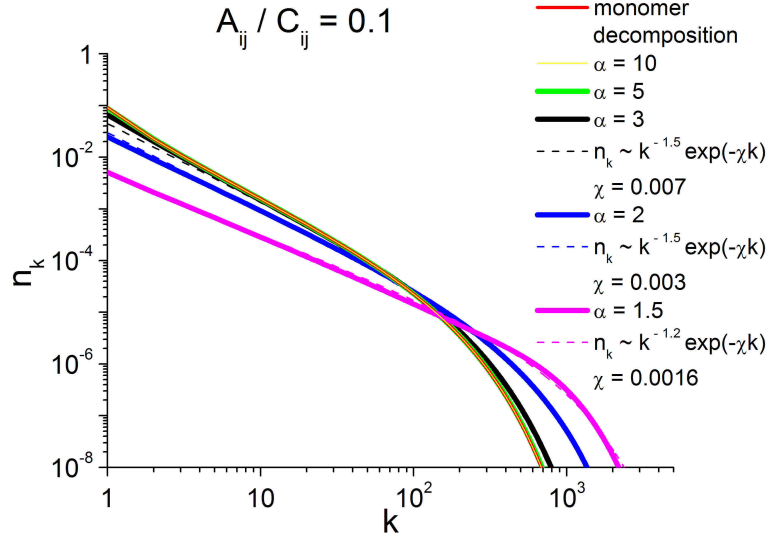


Figure 2: Size distributions for models with a power law distribution of debris sizes  $m_k \sim k^{-\alpha}$  with  $\alpha = 10, 5, 3, 2$ , and  $1.5$  for the case of constant reaction kernel,  $\mu = 0$ . For steep size distributions of the debris,  $\alpha \geq 2$ , the resultant size distribution of aggregates shows practically the same power law and exponential cutoff,  $n_k \sim k^{-3/2} \exp(-\chi k)$ , as the model with a complete disruption into monomers. The parameter  $\chi$ , obtained by fitting, coincides for all  $\alpha = 10, 5, 3$ , and starts to deviate for the frontier value  $\alpha = 2$ , where the exponent of the power-law also starts to differ from  $3/2$ , taking successively descending values.

For the physically relevant distribution in three dimensions the appropriate generalized product kernel (41) has  $\mu = 1/12$  and Eq. 50 implies  $f(R) \sim R^{-11/4}$ . This prediction is in excellent agreement with measurements [22].

As it has been shown above, the exponent  $\mu$  can vary within the interval,  $1/12 \leq \mu \leq 1/3$ , which implies that the exponent  $q$  for the radii distribution obeys the condition,  $2.75 \leq q \leq 3.5$ . Occultation experiments give values for  $q$  in the range from 2.71 to 3.11 [22, 23].

## 4 Calculation of aggregation and fragmentation energies

Here we present estimates for  $E_{\text{agg}}$  and  $E_{\text{frag}}$ . We assume that these quantities are some effective constants which allow an adequate description of the system kinetics in average. All constants below are expressed in SI units and for the notation brevity we skip their dimension.

To estimate the aggregation energy we use the result of [24] for collisions of particles with adhesion. The threshold energy of aggregation reads in this case:

$$E_{\text{agg}} = q_0 \left( \pi^5 \gamma^5 R_{\text{eff}}^4 D^2 \right)^{1/3}. \quad (51)$$

Here  $q_0 = 1.457$  is a constant,  $\gamma$  is the surface tension,  $D = (3/2)(1 - \nu^2)/Y$ , where  $Y$  and  $\nu$  are respectively the Young modulus and Poisson ratio and  $R_{\text{eff}} = R_1 R_2 / (R_1 + R_2)$ . Using material parameters for ice,  $Y = 7 \times 10^9$  Pa,  $\nu = 0.25$ ,  $\gamma = 0.74$  N/m, we obtain  $E_{\text{agg}} = 8.72 \times 10^{-7} R_{\text{av}}^{4/3}$  J, where  $R_{\text{av}}$  is the mean particles radius. The corresponding mean kinetic energy reads,

$$E_{\text{av}} = \frac{1}{2} \left( \frac{4\pi}{3} \phi \rho R_{\text{av}}^3 \right) \bar{V}^2. \quad (52)$$

Here  $R_{\text{av}}$  is the mean aggregate size,  $\rho = 10^3$  kg/m<sup>3</sup> is the ice density and  $\phi$  gives the mean packing fraction of particles, so that  $\phi \rho$  is the actual density of the aggregate. With  $\phi \simeq 0.4$  we obtain,  $E_{\text{av}} = 837.8 R_{\text{av}}^3 \bar{V}^2$  J.

The above Eq. 51 indicates the energy required to separate particles bounded by one adhesive contact. To break a contact of two monomers of radius  $r_0$  the energy of  $E_0 = E_{\text{agg}}(R_{\text{eff}} = r_0/2)$  is needed. To destroy completely an aggregate which has a total number of  $N_c$  adhesive contacts, one needs the energy  $E_{\text{frag}} = N_c E_0$ . The number of contacts equals the number of monomers in the aggregate of size  $R$ , given by  $(4/3)\pi R^3 \phi / ((4/3)\pi r_0^3) =$

$\phi(R/r_0)^3$ , times half the average coordination number  $\bar{n}_c$ . As a result we obtain for the average fragmentation energy,

$$E_{\text{frag}} = 2^{-7/3} q_0 \left( \pi \gamma^5 r_0^4 D^2 \right)^{1/3} \phi \bar{n}_c (R_{\text{av}}/r_0)^3. \quad (53)$$

This yields for  $\bar{n}_c = 4.7$ , found for the random packing of spheres [25, 26]  $E_{\text{frag}} = 8.2 \times 10^{-7} R_{\text{av}}^3 r_0^{-5/3}$  J. Finally, using Eq. 11, we obtain for the coefficient  $\lambda$ :

$$\lambda = \left[ 1 - \left( 1 + \frac{1.04 \times 10^{-9}}{\bar{V}^2 R_{\text{av}}^{5/3}} \right) e^{-\frac{1.04 \times 10^{-9}}{\bar{V}^2 R_{\text{av}}^{5/3}}} \right]^{-1} \exp \left[ -\frac{9.8 \times 10^{-10}}{\bar{V}^2 r_0^{5/3}} \right]. \quad (54)$$

The value of  $R_{\text{av}}$  is to be obtained self-consistently. Namely, we use the so-called "mass-averaged" radius

$$R_{\text{av}} = \frac{\int_{r_0}^{\infty} f(R) R^4 dR}{\int_{r_0}^{\infty} f(R) R^3 dR},$$

which for the distribution (50) yields,

$$R_{\text{av}} = \left[ \frac{\Gamma\left(\frac{5-q}{3}\right)}{\Gamma\left(\frac{4-q}{3}\right)} \right] R_c, \quad (55)$$

where we neglect small terms of the order of  $(r_0/R_c)^4$ . For  $q \approx 3$  we obtain,  $R_{\text{av}} \simeq \left[ \Gamma(\frac{2}{3})/\Gamma(\frac{1}{3}) \right] R_c \simeq 0.506 R_c$ . Using Eq. 50, which relates  $r_0$  and  $\lambda$ , the value of  $R_c = 5.5$  m for the cutoff radius, obtained by fitting to the observational data, and the mean "mass-averaged" radius  $R_{\text{av}} = 0.506 R_c = 2.79$  m, we obtain the following equation, which constrains the monomer radius  $r_0$  for different values of the average random velocity  $\bar{V}$ :

$$\begin{aligned} r_0^{-3/2} &= A \exp(a \bar{V}^{-2} r_0^{-5/3}) \\ A &= c \left[ 1 - \left( 1 + b \bar{V}^{-2} \right) \exp(-b \bar{V}^{-2}) \right], \end{aligned} \quad (56)$$

where  $a = 9.78 \times 10^{-10}$ ,  $b = 1.88 \times 10^{-10}$  and  $c = 0.155$ . Hence Eq. 56 determines the radius of a primary grain for each value of average random velocity  $\bar{V}$ . Solving this equation we find that  $r_0$  ranges from 4.9 cm to 2 mm, when the random velocity  $\bar{V}$  varies from 0.01 cm/s to 0.1 cm/s. In particular, the random velocity  $\bar{V} = 0.03$  cm/s implies a primary grain size of  $r_0 = 1$  cm.

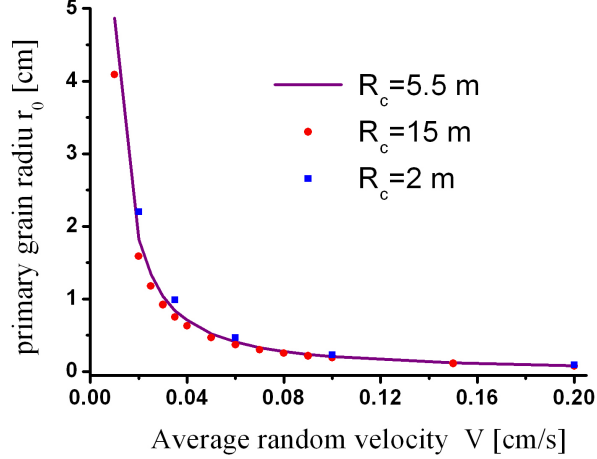


Figure 3: The dependence of the primary grain size  $r_0$  on the chosen value of the average random velocity  $\bar{V}$ . The calculations have been done using Eqs. 56 for  $R_c = 5.5$  m (solid line),  $R_c = 2$  m (squares) and  $R_c = 15$  m (circles). As it may be seen from the figure, different cutoff radii correspond to the same combinations of possible primary grain size and average random velocity. Note that  $R_c$  and  $\bar{V}$  are in fact related additionally by the energy budget of the ring.

Similar calculations may be done for the other value of  $R_c$  – in this case the constants in Eq. 56 read,  $a = 9.78 \times 10^{-10}$ ,  $b = 3.23 \times 10^{-9} R_c^{-5/3}$  and  $c = 2 R_c^{-3/2}$ .

Fig. 3 demonstrates the dependence of the primary grain size  $r_0$  on the chosen value of the average random velocity  $\bar{V}$ . The calculations have been done for  $R_c = 5.5$  m, obtained by fitting to the observational data of [22] and for the two other values of the cutoff radius,  $R_c = 2$  m and  $R_c = 15$  m. It may be seen from the figure that the cutoff radius has practically no impact on the value of  $r_0$  for a given velocity  $\bar{V}$ . Now we can estimate the exponential factor in Eq. 29 of Sec. 2.1.1. Using Eqs. 52 and (53) we find

$$\exp(-E_{\text{frag}}/E_{\text{av}}) = \exp\left(-a r_0^{-5/3} \bar{V}^{-2}\right),$$

where  $a = 9.78 \times 10^{-10}$  and  $r_0$  is to be taken as a function of  $\bar{V}$  from the equation (56). Hence this factor strongly depends on the chosen value of random velocity. For the random velocity interval of  $10^{-4} - 10^{-3}$  m/s we

obtain,

$$4.2 \times 10^{-14} \leq \exp \left[ -a \left( r_0 (\bar{V}) \right)^{-5/3} \bar{V}^{-2} \right] \leq 3.4 \times 10^{-7},$$

that is,

$$4.2 \times 10^{-14} \leq \exp(-E_{\text{frag}}/E_{\text{av}}) \leq 3.4 \times 10^{-7}.$$

## 5 The dependence of the upper cutoff radius $R_c$ on the distance from the planet

Now we discuss the dependence of the upper cutoff radius  $R_c$  on the distance from Saturn  $r$ . According to Eqs. 50 and 11

$$R_c = 2^{2/3} r_0 \lambda^{-2/3} = 2^{2/3} r_0 \left[ 1 - (1 + E_{\text{agg}}/E_{\text{av}}) e^{-E_{\text{agg}}/E_{\text{av}}} \right]^{2/3} e^{2E_{\text{frag}}/3E_{\text{av}}}. \quad (57)$$

Using  $E_{\text{agg}}$  and  $E_{\text{av}}$  found in the previous Section 4 we obtain,

$$E_{\text{agg}}/E_{\text{av}} = 3.26 \times 10^{-9} \bar{V}^{-2} R_c^{-5/3}, \quad (58)$$

which shows that for  $10^{-4} \leq \bar{V} \leq 10^{-3}$  m/s [27, 28] and  $2.4 \leq R_c \leq 11.2$  m [22] the ratio  $E_{\text{agg}}/E_{\text{av}}$  is constrained to the interval  $0.006 \leq E_{\text{agg}}/E_{\text{av}} \leq 0.075$ , that is this ratio is small. Hence one can use in Eq. 57 an expansion in  $E_{\text{agg}}/E_{\text{av}}$  which yields,

$$R_c = 2^{2/3} r_0 (E_{\text{agg}}/E_{\text{av}})^{4/3} e^{2E_{\text{frag}}/3E_{\text{av}}}. \quad (59)$$

Now we relate the average energy of the random motion of particles  $E_{\text{av}}$  to the distance to Saturn. Here we use results of a hydrodynamic analysis of the rings kinetics [29], which from the energy budget of the ring a relation between the Kepler frequency  $\Omega = \sqrt{GM/r^3}$  ( $M$  - is the mass of Saturn,  $G$  - gravitational constant, and  $r$  - the distance to Saturn), diameter of rings particles  $d$ , equatorial packing fraction  $\nu_0$  and average square of random velocity  $T_0$ :

$$\left[ \frac{\Omega d}{\nu_0 \sqrt{T_0}} \right]^2 = \frac{128(1 - \varepsilon^2)(1 + \varepsilon)(3 - \varepsilon)}{5\pi} \frac{\int_0^\infty dz \tilde{\nu}^2 \tilde{T}^{3/2}}{\int_0^\infty dz \tilde{\nu} \tilde{T}}, \quad (60)$$

where  $\varepsilon$  is the restitution coefficient of the ring particles and  $\tilde{\nu} = \nu(z)/\nu_0$  and  $\tilde{T} = T(z)/T_0$  are respectively the reduced  $z$ -dependent packing fraction and mean square random velocity. Using  $R_{\text{av}}$  for  $d$  and  $\bar{V}^2$  for  $T_0$ , we recast this equation into the form,

$$\bar{V}^2 = p_0 \Omega^2 R_{\text{av}}^2 \nu_0^{-2}, \quad (61)$$

where the constant  $p_0$  depends on the restitution coefficient and the vertical distribution of particles. The same relation as (61), but with a different coefficient  $p_0$ , is obtained if one uses a triaxial kinetic approach to the rings dynamics [30]. One expects  $p_0$  on the order of  $0.1 - 0.001^2$ . Using the density of Saturn, equal to  $700 \text{ kg/m}^3$ , the relation  $R_{\text{av}} = 0.506 R_c$  and expressing the distance to Saturn as  $\hat{r} = r/R_s$  ( $R_s$  is the Saturn radius), we obtain,

$$\bar{V} = p_1 R_c \nu_0^{-1} \hat{r}^{-3/2}, \quad (62)$$

with  $p_1 = 2.24 \times 10^{-4} \sqrt{p_0}$ , which together with Eq. 58 yields,

$$E_{\text{agg}}/E_{\text{av}} = p_2 \nu_0^2 R_c^{-11/3} \hat{r}^3, \quad (63)$$

where  $p_2 = 0.0652/p_0$ . Exploiting the relations, derived in the previous Sec. 4 for  $E_{\text{agg}}$  and  $E_{\text{av}}$ , expressed in terms of  $R_{\text{av}}$ ,  $\bar{V}$  and  $r_0$ , and Eq. 62 we find,

$$E_{\text{frag}}/E_{\text{av}} = p_3 \nu_0^2 r_0^{-5/3} R_c^{-2} \hat{r}^3, \quad (64)$$

with  $p_3 = 0.0196/p_0$ . Substituting Eqs. 63 and 64 into Eq. (59) we arrive at the equation for the upper cutoff radius:

$$R_c = B \hat{r}^\beta \exp\left(\alpha \hat{r}^3 / R_c^2\right), \quad (65)$$

where

$$B = \frac{0.583}{p_0^{12/53}} r_0^{9/53} \nu_0^{24/53}, \quad \beta = \frac{36}{53} \simeq 0.68, \quad \alpha = \frac{0.00222 \nu_0^2}{p_0 r_0^{5/3}}$$

The particular quantities in the last equation are determined by the value of  $p_0$ , which depends on the restitution coefficient of particles and the vertical mass and energy distribution in the rings.

---

<sup>2</sup>For instance, for  $\varepsilon = 0.7$  and for the Gaussian approximations  $\tilde{\nu}(z) = \tilde{T}(z) = \exp(-z^2/h^2)$ , where  $h$  is the thickness of the rings, the constant  $p_0$  reads,  $p_0 = 0.0814$ .

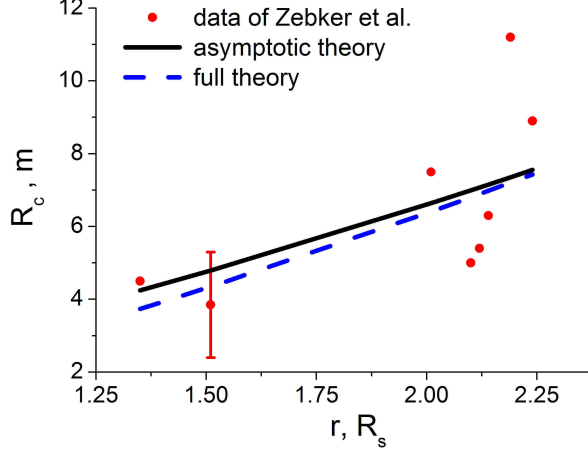


Figure 4: The dependence of the upper cutoff radius  $R_c$  on the distance from Saturn  $r_s$ . Dots represent the observational data taken from table III of [22], for the C ring, Cassini Division, and the A ring. Lines – the prediction of the theory with  $\alpha = 12.56$ . Upper (black) line – the asymptotic theory, Eq. 66, the bottom (blue) line – the full theory, that is, the solution of Eq. 65.

One can find an approximate solution to Eq. 65, depending on the value of  $\alpha \hat{r}^3$ . If  $\alpha^{1/2} \hat{r}^{3/2} \gg 1$  (large density limit) the following approximate expansion holds

$$\begin{aligned}
 R_c &= \frac{\alpha^{1/2} \hat{r}^{3/2}}{\sqrt{\log(\alpha^{1/2} \hat{r}^{3/2}) - \frac{1}{2} \log \left( \alpha^{1/2} \hat{r}^{3/2} - \frac{1}{2} \log \log (\alpha^{1/2} \hat{r}^{3/2} - \dots) \right)}} \\
 &\approx \frac{\alpha^{1/2} \hat{r}^{3/2}}{\sqrt{\log(\alpha^{1/2} \hat{r}^{3/2})}}, \tag{66}
 \end{aligned}$$

where the terms in the "nested" expansion in the above equation are kept, until the argument of the "nested" logarithmic function remains positive.

In the opposite case  $\alpha^{1/2} \hat{r}^{3/2} \ll 1$  we obtain (low density limit),

$$R_c \simeq B \hat{r}^\beta \left( 1 + \alpha/B^2 \hat{r}^{3-2\beta} + \dots \right) \simeq B \hat{r}^{0.68} \left( 1 + \alpha/B^2 \hat{r}^{1.64} + \dots \right) \tag{67}$$

In Fig. 4 the dependence of the upper cutoff radius  $R_c$  on the distance from Saturn is shown together with the theoretical predictions of the full



theory, Eq. 65, and asymptotic theory, Eq. 66, for the parameter  $\alpha = 12.56$ . Although the observational data is very scattered, one can still conclude that the theory adequately describes the observed behavior of  $R_c$ .

## 6 Acknowledgments

This work was supported by Deutsches Zentrum für Luft und Raumfahrt, Deutsche Forschungsgemeinschaft and by Russian Foundation for Basic Research (RFBR, project 12-02-31351). Numerical calculations were performed using Chebyshev supercomputer of Moscow State University.

## References

- [1] Brilliantov, N. V., Bodrova, A. S. & Krapivsky, P. L. A model of ballistic aggregation and fragmentation. *Journal of Statistical Mechanics: Theory and Experiment* **P06011**, 1–18 (2009).
- [2] Bodrova, A., Schmidt, J., Spahn, F. & Brilliantov, N. Adhesion and collisional release of particles in dense planetary rings **218**, 60–68 (2012).
- [3] Brilliantov, N. V. & Pöschel, T. *Kinetic Theory of Granular Gases* (Oxford University Press, Oxford, 2004).
- [4] van Noije, T. & Ernst, M. H. *Granular Matter* **1**, 57 (1998).
- [5] Garzo, V. & Dufty, J. W. *Phys. Rev. E* **59**, 5895 (1999).
- [6] Spahn, F., Albers, N., Sremcevic, M. & Thornton, C. Kinetic description of coagulation and fragmentation in dilute granular particle ensembles. *Europhysics Letters* **67**, 545–551 (2004).
- [7] Brilliantov, N. V. & Spahn, F. *Mathematics and Computers in Simulation* **72**, 93 (2006).
- [8] Colwell, J. E. *et al.* *The Structure of Saturn’s Rings*, 375 (Springer, 2009).
- [9] Salo, H. Gravitational wakes in Saturn’s rings. *Nature* **359**, 619–621 (1992).

- [10] Colwell, J. E., Esposito, L. W. & Sremcevic, M. Self-gravity wakes in saturn's a ring measured by stellar occultations from cassini. *Geophysical Research Letters* **33**, L07201 (2006).
- [11] Hedman, M. *et al.* Self-gravity wake structures in saturn's a ring revealed by cassini vims. *Astronomical Journal* **133**, 2624–2629 (2007).
- [12] French, R. G., Salo, H., McGhee, C. A. & Dones, L. H. Hst observations of azimuthal asymmetry in saturn's rings. *Icarus* **189**, 493–522 (2007).
- [13] Toomre, A. On the gravitational stability of a disk of stars. *Astrophys. J.* **139**, 1217–1238 (1964).
- [14] Wisdom, J. & Tremaine, S. Local simulations of planetary rings. *Astron. J.* **95**, 925–940 (1988).
- [15] Araki, S. & Tremaine, S. The dynamics of dense particle disks. *Icarus* **65**, 83–109 (1986).
- [16] Résibois, P. & De Leener, M. *Classical kinetic theory of fluids* (Wiley & Sons, New York, 1977).
- [17] Jeffreys, H. The relation to cohesion to roche's limit. *Mon. Not. Roy. Astron. Soc.* **107**, 260–262 (1947).
- [18] Johnson, K. L., Kendall, K. & Roberts, A. Surface energy and the contact of elastic solids. *Proc. R. Soc. Lond. A* **324**, 301 (1971).
- [19] Guimaraes, A. H. F. *et al.* How adhesion influences the growth and resistivity of aggregates in saturns rings. *Icarus* **submitted** (2011).
- [20] Srivastava, R. C. *J. Atom. Sci.* **39**, 1317 (1982).
- [21] Hayakawa, H. *Master Thesis, Kobe University* (1988).
- [22] Zebker, H. A., Marouf, E. A. & Tyler, G. L. Saturn's rings - Particle size distributions for thin layer model. *Icarus* **64**, 531–548 (1985).
- [23] French, R. G. & Nicholson, P. D. Saturn's Rings II. Particle sizes inferred from stellar occultation data. *Icarus* **145**, 502–523 (2000).

- [24] Brilliantov, N. V., Albers, N., Spahn, F. & Pöschel, T. Collision dynamics of granular particles with adhesion. *Phys. Rev. E* **76**, 051302 (2007).
- [25] Brilliantov, N. V. e. a. Effective mechanical properties of aggregates built up by randomly packed adhesive spheres. *preprint* (2011).
- [26] Peters, E. A., Kollmann, M., Barenbrug, T. M. & Philipse, A. P. Caging of a d-dimensional sphere and its relevance for the random dense sphere packing. *Phys. Rev. E* **63**, 021404 (2001).
- [27] Schmidt, J., Ohtsuki, K., Rappaport, N., Salo, H. & Spahn, F. *Dynamics of Saturn's Dense Rings*, 413–458 (Springer, 2009).
- [28] Cuzzi, J. N. *et al.* An Evolving View of Saturn's Dynamic Rings. *Science* **327**, 1470–1475 (2010).
- [29] Schmidt, J., Salo, H., Petzschmann, O. & Spahn, F. Vertical distribution of temperature and density in a planetary ring. *Astronomy and Astrophysics* **345**, 646–652 (1999).
- [30] Simon, V. & Jenkins, J. On the vertical structure of dilute planetary rings. *Icarus* **110**, 109–116 (1994).